Analyst

PAPER

View Article Online
View Journal | View Issue

Cite this: *Analyst*, 2014, **139**, 3115

A real time affinity biosensor on an insulated polymer using electric impedance spectroscopy in dielectric microchips†

Mohammed Kechadi,[abc] Bruno Sotta,[d] Lila Chaal,[c] Bernard Tribollet[ab] and Jean Gamby*[ab]

Received 28th January 2014
Accepted 20th March 2014

DOI: 10.1039/c4an00212a

www.rsc.org/analyst

This paper presents development of real time monitoring of binding events on flexible plastic in microchips. Two planar carbon microelectrodes are integrated into an insulated polyethylene terephthalate microchip without direct electrical contact with the solution in the microchannel. It has been possible to probe the electric impedance changes through the interface constituted by the microelectrode/PET microchannel/solution when a biomolecular interaction takes place on the polymer surface. This new transduction for biosensing was demonstrated for the molecular recognition of BSA immobilized on the polymer microchannel surface using the corresponding rabbit anti-BSA antibodies as an analyte in the flow microchannel at the nanomolar range concentration. The equilibrium association constant was determined for the affinity reaction between both ligands and was obtained equal to 5×10^7 M^{-1}. The promising results obtained with this new device make it a competitive biosensor.

1 Introduction

The last decades have seen the emergence of microfluidic devices with various tranducers for affinity biosensor development. The most used tranducers are electrochemical,[1,2] electroacoustic,[3,4] or optical[5,6] for detecting interactions between ligands. Surface plasmon resonance (SPR) is one of the most used optical biosensors for the measurement of the refractive index changes.[7,8] As illustrated in Fig. 1A with the Biacore SPR instrument scheme, the ligand (antigen, receptor…) is immobilised in the hydrogel, while the analyte (antibody, messenger…) flows in the channel and diffuses in the gel where the ligand is bound. The metal/dielectric interface constituting a glass slide coated with hydrogel and gold is excited by a beam of monochromatic light, under conditions of total reflection leading to the resonance. The light beam probes the hydrogel and detects changes in the local refractive index due to the accumulation of analyte mass. The depth of the evanescent wave is 100 nm towards the hydrogel, *i.e.* the thickness of the hydrogel itself.

In the last decades, several groups have focused on electrical signal transduction in the microchip by using the direct or indirect electrode configuration to measure the conductivity of the streaming electrolyte in the microchannel. An original technique has been the development of measurements through capacitively coupled contactless conductivity detection (C^4D) through two electrodes with a distance separation constituting the detector cell.[9–11] However, the high applied ac voltage 0.5–10 V amplitudes are much larger than conventionally used values, 5–100 mV. Such large amplitude generates a non-linear relationship between the voltage and current which causes distortion of impedance results. It is for this reason that this transduction can be viewed as a pseudoimpedance or transimpedance technique.

In recent years, the laser photoablation technique was used to define a well-controlled microelectrode position in the polymer microchip. The feeble gap between the microelectrodes as well as with the thin layer of the dielectric material that coated the microelectrode allowed the avoidance of the linearity problem.[12] As mentioned for SPR, the principle of the developed electric impedance in the dielectric microchip is also based on the metal/dielectric interface excitation by applying a modulated voltage of one hundred of millivolts in frequency range through the dielectric layer. The output impedance through the device can thus be related to the interfacial impedance of the modified dielectric layer sandwiched between the microelectrodes and the flow microchannel (see Fig. 1B). The crucial advantage of electric impedance spectroscopy on an insulated polymer sandwiched between two microelectrodes is the absence of direct contact between the microelectrodes and the

[a]*CNRS, UMR 8235, Laboratoire Interface et Systèmes Electrochimiques, (LISE), F-75005 Paris, France. E-mail: Jean.gamby@upmc.fr*

[b]*Sorbonne Universités, UPMC Univ Paris 06, UMR 8235, Laboratoire Interfaces et Systèmes Electrochimiques, (LISE), 4 Place Jussieu, F-75005, Paris, France*

[c]*Laboratoire d'Electrochimie, Corrosion et de Valorisation Energétique (LECVE), Faculté de Technologie, Université A. MIRA, Béjaia 06000, Algeria*

[d]*Sorbonne Universités, UPMC Univ Paris 06, UMR 7622, Laboratoire Biologie des Semences, 4 Place Jussieu, F-75005 Paris, France*

† Electronic supplementary information (ESI) available. See DOI: 10.1039/c4an00212a

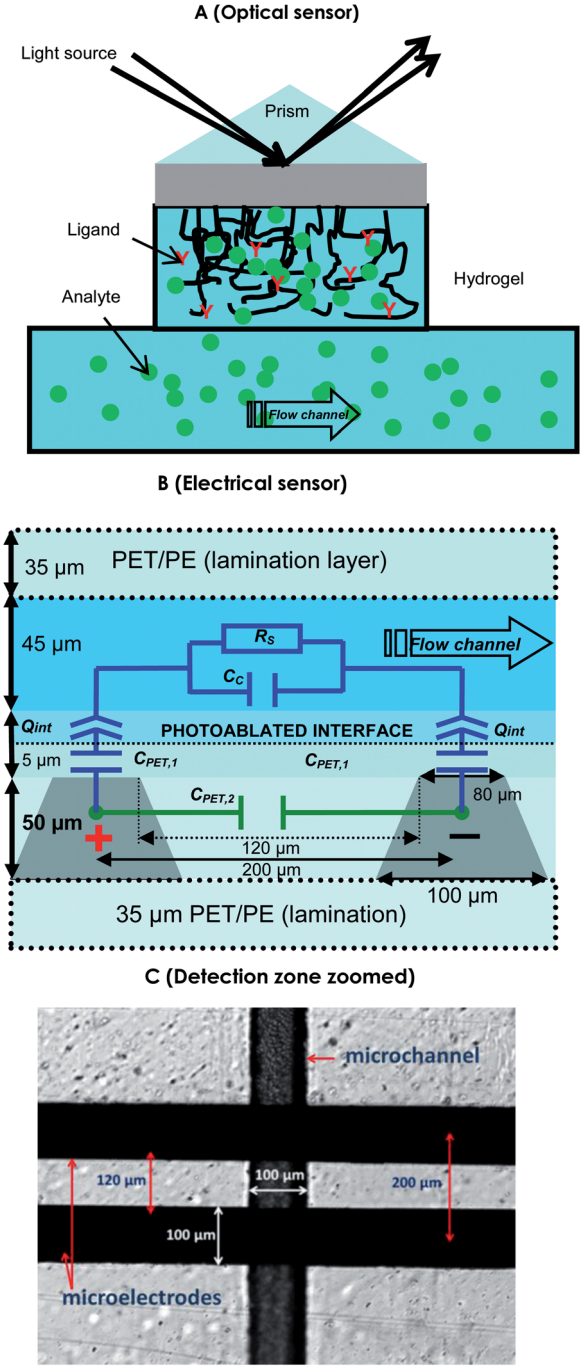

Fig. 1 (A) Schematic representation of the BIACORE optical biosensor. The hydrogel is 100 nm high approximately; the flow channel for a standard instrument is 24 mm long, 50 μm high and 500 μm width. The ligand is immobilised in the hydrogel, the analyte flows in the channel and diffuses in the gel where it binds to the ligand. (B) Cross-section of the dielectric interface microelectrode/PET/microchannel and the corresponding electrical equivalent circuit: $C_{PET,2}$ for the 120 μm PET layer impedance (distance separation), $C_{PET,1}$ for the 5 μm PET layer impedance (non-contact layer thickness), the element CPE, Q_{int}, for the interfacial impedance (photoablated surface), and the parallel association of the solution resistance, R_S, and the cell capacitance, C_C. Please note that for a more detailed view of the interface the dimensions are not to scale. (C) The zoomed detection is taken under an inverted microscope.

flow microchannel.[12,13] As a consequence the polymer microchannel layer sandwiched between the two planar microelectrodes can be considered as a dielectric component[14] whose physical properties may change in response to an external electrical excitation. Based on this principle, in a previous paper, a flow sensor was developed to record at a high fixed frequency the chemical conversion of enzymatic substrates like aminophenyl phosphate in the PET microchannel through the channel resistivity.[15] In this paper, we demonstrate for the first time the possibility to probe the interfacial electric impedance change when a biomolecular interaction takes place between a ligand in solution (analyte) and a ligand attached onto the polymer microchannel. This new transduction for biosensing was demonstrated for the detection and quantification of bovine serum albumin (BSA) immobilized on the polymer microchannel surface using the corresponding rabbit anti-BSA antibodies (Ab-BSA) as an analyte, which is loaded in the flow microchannel at the nanomolar range concentration. Experimental studies are based on the real time monitoring of the measured impedance variation at a fixed frequency (400 Hz) by applying a small 100 mV alternating potential excitation through two microband electrodes, during the association/dissociation rate between Ab-BSA loaded in the flow microchannel and BSA immobilized on PET.

2 Materials and methods

2.1 Chemicals

10 mM of tris(hydroxymethyl)aminomethane (from Sigma Aldrich) was obtained after dilution in 10 mM HCl and 10 mM NaCl. The checked pH was at 9 and was used as the buffer solution. 1 mM NaOH (from Sigma Aldrich) was used as the washing buffer in a regenerating step. Bovine serum albumin (96%) was purchased from VWR International. The rabbit anti-bovine serum albumin antibodies (Ab-BSA) were received from Sigma-Aldrich. The antibody solutions were also diluted in the buffer solution from a 10^{-5} M Ab-BSA stock solution in 50% glycerol. Tween 20 solution was used with the ratio: Tween 20/buffer solution = 0.2 mL L^{-1}.[16]

2.2 Microchannel networks

The photoablation procedure for the microchannel networks has been previously described.[12,17] In brief, the microchip used in this work was realised by the photoablation process which leads to the ablation of the material in contact with the UV laser source. Before the photoablation step, the PET film thickness was measured to be 100 μm. On the one side of the PET sheet two parallel microchannels (which will be transformed into microelectrodes) were drilled. The two microchannels depth into the PET film was measured under a microscope at 50 μm. On the other side of the PET sheet, a perpendicular microchannel for fluidic devices was drilled having a trapezoidal cross-section shape with a depth of 45 μm, a width of 100 μm and a length of 1.4 cm (see Fig. 1B and C). Thus, a 5 μm thick PET layer separated the microchannel from the bottom of the two microelectrodes (see Fig. 1B). The two parallel

microchannels were transformed into microelectrodes by the incorporation of a graphite carbon ink and then dried afterward at 50 °C. Finally the photo-ablated PET film was laminated using a 35 μm PE/PET layer. As shown in Fig. 1B and C, the distance separation between both microelectrodes is 120 μm edge to edge (200 μm center to center) and the detection surface area per microelectrode is 80 μm × 100 μm. A study was carried out by the electric impedance measurement in alternative mode (ac) through the two microelectrodes at the frequency range from 1 MHz to 1 Hz with 0.1 V amplitude, in order to control the dielectrical behaviour of the overall microsystem and to extract the specific microchannel response from the background response.[18]

2.3 Instrumentation

Impedance measurements are performed using a dielectric interface (Solartron, DI 1260) gain phase impedance analyzer coupled with a frequency response analyzer (Solartron, FRA 1255). The dielectric interface is characterised by the large frequency range, from 1 mHz to 20 MHz. Software Smart (Solartron Analytical) was used as the computer control of all experimental set-up. The dielectric interface is usually used for high impedance measurements on a highly insulated material that is the case with polyethylene terephthalate. Indeed, the current measurement range of the system varies from 6 mA to 100 fA, thus enabling the measurement of a very high impedance (100 Ω to 100 TΩ). In this study, the impedance measurement is performed at a low fixed-frequency (here 400 Hz) which was appropriate for sensing the interfacial impedance through the dielectric microchip device connected to a dielectric interface apparatus.

2.4 Experimental procedure for electric impedance measurements in the dielectric microchip

The microchip characteristics with an insulated PET layer sandwiched between two galvanic isolated microelectrodes can be assimilated to a dielectric interface with, on the one part of the 5 μm PET thin polymer layer, electronic charges on microelectrodes and, on the other part, ionic charges in the microchannel considering impedances for each part of the microchip (see Fig. 1B).

The global impedance $Z_G(\omega)$ between the two microelectrodes with a filled microchannel depends on the different parts which constitute the microchip. In this configuration, $Z_G(\omega)$ can be expressed as the combination between $Z_1(\omega)$ (blue line in Fig. 1B) and $Z_2(\omega)$ (green line in Fig. 1B)[18] as follows,

$$Z_G(\omega)^{-1} = Z_1(\omega)^{-1} + Z_2(\omega)^{-1} \quad (1)$$

Firstly, acquisition and interpretation of electric impedance are performed with an empty microchannel through a 100 mV voltage excitation applied between the two carbon microelectrodes embedded in PET and separated to 200 μm center to center (120 μm edge to edge, Fig. 1B). The 120 μm PET impedance layer, $Z_2(\omega)$, which separated two electrodes, behaves as a capacitor (see eqn (2)) and will be eliminated from the global impedance, $Z_G(\omega)$, in further experiments when the microchannel will be filled. The capacitance written in eqn (2) was obtained as $C_{PET,2} = 8 \times 10^{-13}$ F.

$$Z_2(\omega) = \frac{1}{j\omega C_{PET,120\mu m}} \quad (2)$$

where ω is the angular frequency (rad s^{-1}), defined by $\omega = 2\pi f$, where f is the frequency.

The target application is the real-time monitoring of the electric impedance module variation $Z_1(\omega)$ at low frequencies. The latter impedance as shown in Fig. 1B corresponds to a serial combination of three impedances as written below:

$$Z_1(\omega) = 2Z_{1,PET}(\omega) + 2Z_{int}(\omega) + Z_{microchannel}(\omega) \quad (3)$$

The first term in eqn (3) is the 5 μm PET layer impedance from the top of one electrode to the channel bottom that behaves also as $C_{PET,120\mu m}$ (see eqn (2)). The value of $C_{PET,5\mu m}$, equals 14×10^{-11} F, is fixed and will be suppressed during the normalized procedure. The second term shown in eqn (3) is the microchannel solution impedance, Z_S, that corresponds to a parallel association between the microchannel solution resistivity, R_S, and the cell capacitance, C_C. The resistance R_S only depends on the buffer concentration that is high in comparison with the analyte concentration. The capacitance, C_C, is defined as a geometric capacitor that only depends on the chip dimension. The latter was equal to $C_C = 3 \times 10^{-13}$ F. The last term represents the interfacial impedance, Z_{int}, at the photoablated PET/solution interface. As obtained in previous paper,[19] the latter behaves as a non-ideal capacitance represented by a constant phase element (CPE) where α_{int} and Q_{int} are the CPE exponent and the CPE element (see eqn (4)), respectively.

$$Z_{int}(\omega) = \frac{1}{(j\omega)^{\alpha_{int}} Q_{int}} \quad (4)$$

To conclude, Z_{int} is the only interesting parameter to monitor (see eqn (3)) which varies when a biomolecular interaction takes place on the photoablated PET surface throughout the course of the experiment. As a consequence, the real time monitoring of Z_{int} can be measured through the relative variation of Z_1. Indeed, the latter at low frequencies mainly reflects the contribution of the interfacial impedance as written in eqn (5).

$$\Delta Z_1(\omega) = \Delta Z_{int} \quad (5)$$

2.5 Experimental procedure for adsorption monitoring

In the first step, the PET microchannel was coated under a laminar flow containing 10^{-7} M BSA for 1200 s in order to saturate the microchannel surface. The solutions were loaded into the microchannel using a high precise micropump with a flow rate equal to $F_v = 7.2$ μL min^{-1}. Indeed this optimized BSA concentration was chosen because it corresponds to the experimental plateau for BSA adsorbed onto the PET surface.[20] Before loading the antibody, Tween 20 solution was also introduced over 1200 s to prevent the non-specific adsorption of Ab-BSA in

the molecular recognition step.[16] The molecular recognition step was the introduction of various Ab-BSA solution (concentrations from 10^{-8} to 10^{-7} M) under the same hydrodynamic conditions. The last step consisted in a washing procedure with 10^{-3} M NaOH for PET surface regeneration.[20–22] This procedure allows the start baseline recovering when water and the buffer solution were introduced again for a new started run experiment.

3 Results and discussion

3.1 Affinity reaction rate determination on the PET microchannel

A typical variation of the interfacial impedance module when Ab-BSA solution is loaded on a prepared PET microchannel surface (BSA then Tween 20) is shown in Fig. 2. The initial value corresponds to the electric impedance module baseline obtained after BSA and Tween 20 samples were successively loaded in the microchannel (named Z_{BSA}). First, a control experiment was performed showing no significant changes in the measured interfacial impedance modulus when no rabbit anti-BSA antibodies are present in buffer solution (Fig. 2, curve a). Secondly, the measured interfacial impedance modulus increases in the presence of Ab-BSA diluted with the buffer solution when the affinity reaction with BSA takes place. Then, the interfacial impedance signal response reaches a plateau value corresponding to a stationary signal (named $Z_{Ab\text{-}BSA}$). A statistical study about the changes in the interfacial impedance modulus in the presence of Ab-BSA is given in Table S1 (see the ESI†).

The difference between the two stationary signals leads to an equilibrium status named $\Delta Z_{Ab\text{-}BSA,eq}$ which is equal to $Z_{BSA} - Z_{Ab\text{-}BSA}$. Plotting the equilibrium binding obtained from the difference values $\Delta Z_{Ab\text{-}BSA,eq}$ against various loaded Ab-BSA concentrations leads to an isotherm behaviour shown in Fig. 3A. Indeed, as the reaction binding progresses, the rate decreases gradually until a state that corresponds to an equilibrium between association and dissociation rates. The maximum value obtained for $\Delta Z_{Ab\text{-}BSA,eq}$ is more quickly reached when the Ab-BSA concentration is high. We obtained a maximum value of $\Delta Z_{Ab\text{-}BSA,eq}$ (named $\Delta Z_{Ab\text{-}BSA,max}$) from an Ab-BSA concentration equals to 5×10^{-8} M. This means that all the active sites of BSA molecules adsorbed onto the PET microchannel are saturated after the biomolecular recognition with Ab-BSA.

In order to find the model parameters corresponding to the binding reaction between Ab-BSA and BSA determined by impedance measurements, the relative equilibrium binding curve is plotted against the Ab-BSA concentration after normalization of $\Delta Z_{Ab\text{-}BSA,eq}$ values divided by $\Delta Z_{Ab\text{-}BSA,max}$

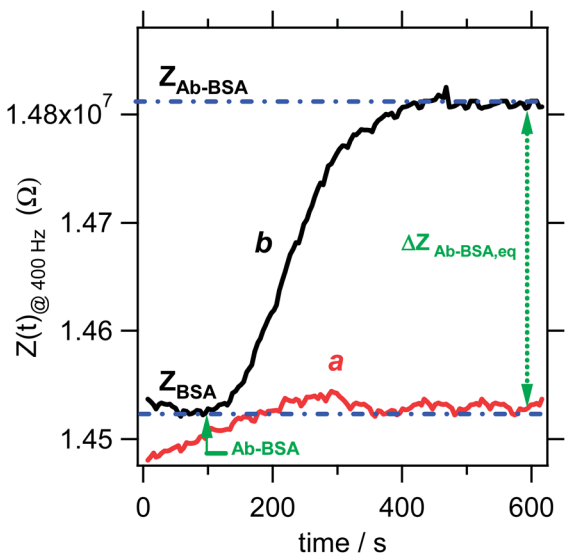

Fig. 2 Sensorgrams showing the impedance module *versus* time. Curve a: a control experiment when no rabbit anti-BSA antibodies are present in buffer solution. Curve b: the association step between Ab-BSA as an analyte and the adsorbed BSA on the microchannel sensor at a fixed frequency of 400 Hz and for a flow rate of 7.2 μL min^{-1}. Step 1: BSA and Tween 20 in buffer solution for microchannel coating. Step 2: introduction of 4×10^{-8} M Ab-BSA diluted in the buffer solution.

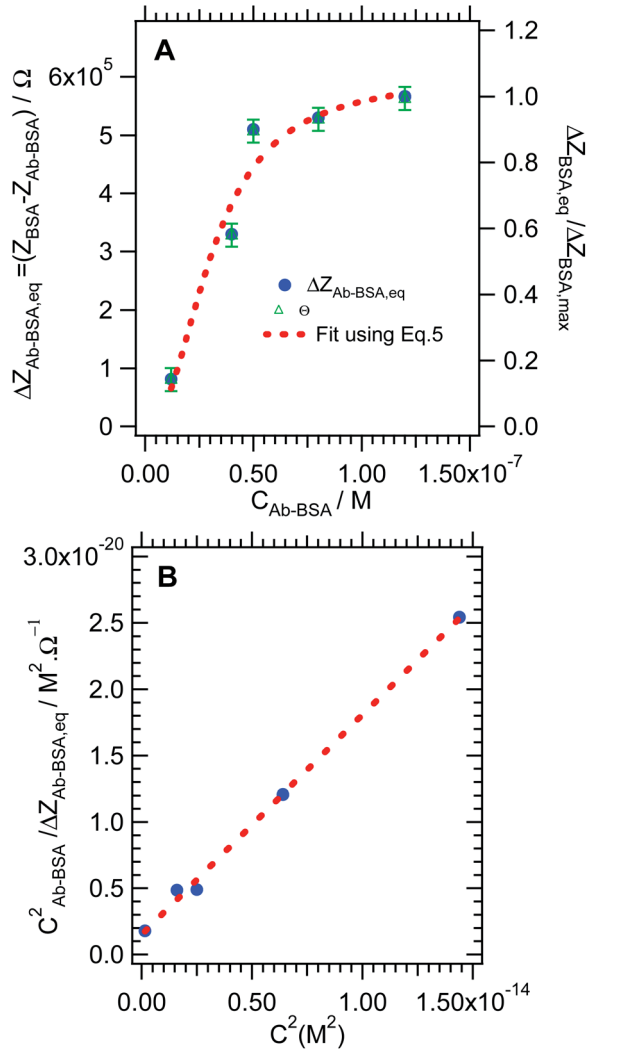

Fig. 3 Calibration curves obtained for various Ab-BSA concentrations loaded on the coated PET surface with BSA. (A) An association isotherm of Ab-BSA on the adsorbed BSA obtained from various experimental sensorgrams from 12 nM to 120 nM concentration. (B). Linearization step of the association isotherm using a linear fit as shown in eqn (7).

(shown in the right-axis of Fig. 3A). As described previously, for Ab-BSA concentrations lower than 5×10^{-8} M, the equilibrium binding varies linearly. The Langmuir equation model[23] has been tested to fit the experimental data presented in Fig. 3 without good correlation. However, as yet known for heterogeneous sites for adsorption, the adapted Langmuir model named the Langmuir–Freundlich model[20,24,25] was more adequate for the fitting procedure to determine the kinetics parameters.

Briefly, in the described experiment, the impedance normalized in Fig. 3B was assumed to be in linear correlation with the surface concentration of occupied sites. As a consequence, the Langmuir–Freundlich combined expression can be expressed as follows in eqn (6):

$$\theta\left(C^{m}_{\text{Ab-BSA}}\right) = \frac{\Delta Z_{\text{Ab-BSA,eq}}}{\Delta Z_{\text{Ab-BSA,max}}} = \frac{K^{\text{app}}_{\text{BSA/Ab-BSA}} C^{m}_{\text{Ab-BSA}}}{1 + \left(K^{\text{app}}_{\text{BSA/aAb-BSA}} C^{m}_{\text{Ab-BSA}}\right)} \quad (6)$$

where θ ($C^{m}_{\text{Ab-BSA}}$) can be viewed as the capacity of the microchannel to reach the maximum coverage, m exponent represents the power term of Freundlich, and the apparent equilibrium constant, $K^{\text{app}}_{\text{BSA/Ab-BSA}}$.

As traditionally admitted for the Langmuir equation,[23] a linear expression of eqn (6) is a useful test for the model validation as shown in eqn (7):

$$\frac{C^{m}_{\text{Ab-BSA}}}{\Delta Z_{\text{Ab-BSA,eq}}} = \frac{1}{K^{\text{app}}_{\text{BSA/Ab-BSA}} \Delta Z_{\text{Ab-BSA,max}}} + \frac{C^{m}_{\text{Ab-BSA}}}{\Delta Z_{\text{Ab-BSA,max}}} \quad (7)$$

In order to obtain the traditional unit in M^{-1} for the equilibrium constant $K_{\text{BSA/Ab-BSA}}$ the following relation must be taken into account:

$$K^{\text{app}}_{\text{BSA/Ab-BSA}} = \frac{K_{\text{BSA/Ab-BSA}}}{[\text{Ab-BSA}]} \quad (8)$$

As predicted, a better fit of experimental data is obtained with the Langmuir–Freundlich equation and the obtained parameters are equal to $K^{\text{app}}_{\text{BSA/Ab-BSA}} = 5 \times 10^{15}\ \text{M}^{-2}$ and $m = 2$.

By replacing eqn (8) in eqn (6) and (7), we recover the typical Langmuir equation model with a power term corresponding to the unit ($m = 1$). The linearization step of the association isotherm using a linear fit as shown in eqn (7) leads to a straight line with a correlation coefficient R^2 equals to 0.996. Indeed, the curve fitting highlights a straight line characterized by a slope of $1.65 \times 10^{-6}\ \Omega^{-1}$ and an intercept of $1.51 \times 10^{-21}\ \text{M}^2\ \Omega^{-1}$. From these values the parameters of eqn (6) were obtained equal to $m = 2$, $\Delta Z_{\text{Ab-BSA,max}} = 0.606\ \text{M}\Omega$ and $K^{\text{app}}_{\text{BSA/Ab-BSA}} = 1.1 \times 10^{15}\ \text{M}^{-2}$.

3.2 Kinetic model for the affinity reaction on the polymer microchannel

The interaction model for the binding reaction between Ab-BSA and BSA can be defined in the following reaction scheme:

$$\text{BSA}_{\text{ads}} + (\text{Ab-BSA})_{\text{solution}} \underset{k_{\text{off}}}{\overset{k_{\text{on}}}{\Leftrightarrow}} (\text{BSA}_{\text{ads}} - (\text{Ab-BSA}))_{\text{associated}}$$

As demonstrated previously, the results involve the fact that the observed association rate, v_{obs}, between Ab-BSA and BSA can be expressed as a second order reaction proportional to the square of Ab-BSA concentration, as follows:

$$v_{\text{obs}} = k_{\text{obs}}[\text{Ab-BSA}]^2 \quad (9)$$

with v_{obs} in M s^{-1} and k_{obs} in $\text{M}^{-1}\ \text{s}^{-1}$ representing the observed association kinetic rate constant.

Taking into account the concentration influence in the observed second order, the association kinetic rate constant can be determined as follows:

$$k_{\text{on}} = k_{\text{obs}}[\text{Ab-BSA}] \quad (10)$$

with k_{on} in s^{-1}.

The dissociation rate of the BSA_{ads}–(Ab-BSA) complex, v_{off}, is proportional to the BSA_{ads}–(Ab-BSA) concentration and it is considered as a zero order reaction since the amount of the adsorbed complex BSA_{ads}–(Ab-BSA) on the PET microchannel can be considered as a constant:

$$v_{\text{off}} = k_{\text{off}} \quad (11)$$

with k_{off} in M s^{-1} representing the dissociation kinetic rate constant.

As a consequence the ratio ($k_{\text{on}}/k_{\text{off}}$) is defined as the equilibrium constant, $K_{\text{BSA/Ab-BSA}}$ which is defined in M^{-1}.

The aim is now to determine, by a full fitting procedure of the sensorgram impedance curve (see Fig. 2), the kinetic parameters k_{on} and k_{off} leading to an estimation of the equilibrium constant of the complex BSA_{ads}–(Ab-BSA). For that, a theoretical expression of the impedance module $Z(t)$ at fixed frequencies with time can be written taking into account the

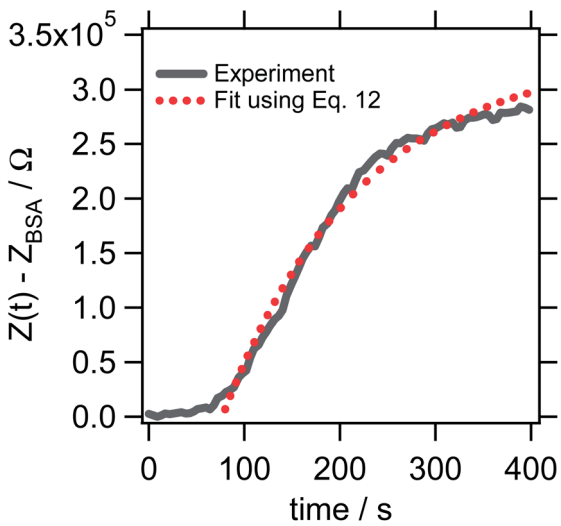

Fig. 4 Experimental and fitted sensorgrams of the interfacial impedance modulus for 4×10^{-8} M of Ab-BSA loaded in the flow microchannel sensor showing the association reaction between Ab-BSA and the adsorbed BSA at a fixed frequency of 400 Hz and for a flow rate of 7.2 μL min^{-1}. The curve fit was performed with eqn (12) leading k_{on}, k_{off} equal to $8.56 \times 10^{4}\ \text{s}^{-1}$ and $3 \times 10^{-3}\ \text{M s}^{-1}$, respectively.

fact that the initial amount of BSA adsorbed is related to impedance Z_{BSA} at the time $t = 0$, as follows:

$$Z(t) - Z_{BSA} = \Delta Z_{Ab\text{-}BSA,max}\left(\frac{k_{on}C_{Ab\text{-}BSA}}{k_{on}C_{Ab\text{-}BSA} + k_{off}}\right) \times \left[1 - \exp\left(-\left(k_{on}C_{Ab\text{-}BSA} + k_{off}\right)t\right)\right] \quad (12)$$

where $Z(t)$ in Ω is the impedance module measured at a fixed frequency of 400 Hz.

The result of the fitting procedure using eqn (12) is illustrated in Fig. 4 with a working Ab-BSA concentration taken as 4×10^{-8} M^{-1}. The obtained values of k_{on} and k_{off} are 8.56×10^4 s^{-1} and 3×10^{-3} M s^{-1} respectively. The same procedure was applied for various Ab-BSA concentrations and values of k_{on} and k_{off} have been determined for each curve (see Table S2 in the ESI†). All the kinetic data obtained are presented in Fig. 5A. It can be noticed that the values of k_{on} and k_{off} are slightly dependent on the Ab-BSA concentration while the ratio, k_{on}/k_{off}, is, as expected, less dependent on the Ab-BSA concentration, as shown in Fig. 5B. The latter underlines that an average value for $K_{BSA/Ab\text{-}BSA}$ can be estimated as $(5.15 \pm 1.45) \times 10^7$ M^{-1}, that is in a good agreement with the literature.[26] It is observed that the average value is very close to the one obtained with the higher Ab-BSA concentration *i.e.* 1.2×10^7 M^1.

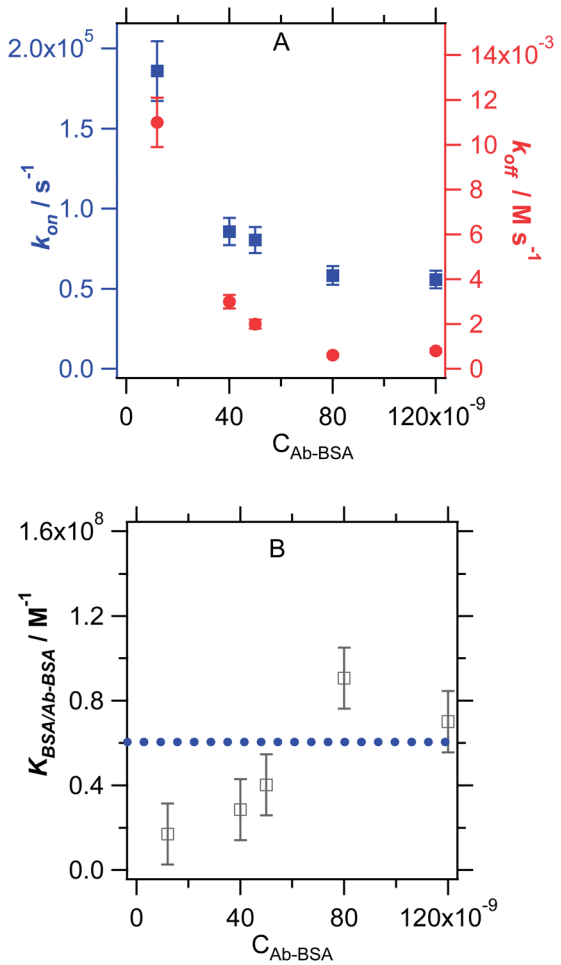

Fig. 5 Kinetic parameters obtained from the fitted sensorgrams of the interfacial impedance modulus with several Ab-BSA (from 1.2×10^{-8} to 1.2×10^{-7}) loaded in the flow microchannel sensor coated with BSA. (A) The values obtained were from the fitting procedure using eqn (12) leading k_{on} and k_{off} parameters which appear on the left-axis and right-axis, respectively. (B) The equilibrium constant corresponding to each k_{on}/k_{off} ratio is shown for each Ab-BSA concentration (see Table 2 in the ESI†).

4 Concluding remarks

Electric impedance spectroscopy in the microchip was applied for the first time to monitor the biomolecular recognition of two ligands on an insulated polymer designed as a microchip. As shown, the presence of BSA molecules immobilized on the microchannel detection zone increases the interfacial impedance module leading to a sensitive surface for biosensing in the nanomolar range concentration. The high sensitivity is found because this transduction takes advantage of the dielectric properties of the flow microchannel embedded in PET with two planar microband electrodes without contact with the solution, thus avoiding non-specific adsorption on microelectrodes and degradation of biological samples through uncontrolled Faradic reactions. Experimental results obtained highlight the possibility for the monitoring at low fixed-frequency of the electric impedance changes provoked by the association of protein ligands. Here it is illustrated for the association reaction between rabbit anti-BSA antibodies in solution and BSA adsorbed onto the PET surface. Thus, it was found that the kinetics of association reaction rate depends on a second order kinetic law with the anti-BSA antibodies concentration. The promising results obtained for the kinetic parameters and the equilibrium association constants between ligands using the present methodology make it a competing method for biosensing. The dielectric PET microchip is also a low cost and flexible material which offers a multiuse chip possibility. It could be used to screen putative partners in biological fluids with regard to a specific protein. Also, the minute volumes of solvent used make it suitable as a detector for a capillary electrophoresis apparatus or to be connected with a mass spectrometer.

Acknowledgements

The authors thank Prof Hubert Girault and Dr Philippe Flückiger for allowing them access to experimental facilities at the EPFL center of MicroNano Technology, Lausanne.

Notes and references

1 A. Qureshi, Y. Gurbuz, S. Kallempudi and J. H. Niazi, *Phys. Chem. Chem. Phys.*, 2010, **12**, 9176–9182.
2 N. J. Ronkainen, H. B. Halsall and W. R. Heineman, *Chem. Soc. Rev.*, 2010, **39**, 1747–1763.
3 J. Gamby, M. Lazerges, C. Pernelle, H. Perrot, H. H. Girault and B. Tribollet, *Lab Chip*, 2007, **7**, 1607–1609.
4 R. Schirhagl, U. Latif, D. Podlipna, H. Blumenstock and F. L. Dickert, *Anal. Chem.*, 2012, **84**, 3908–3913.
5 R. Davidsson, B. Johansson, V. Passoth, M. Bengtsson, T. Laurell and J. Emneus, *Lab Chip*, 2004, **4**, 488–494.

6 F. B. Myers and L. P. Lee, *Lab Chip*, 2008, **8**, 2015–2031.
7 J. Homola, *Anal. Bioanal. Chem.*, 2003, **377**, 528–539.
8 A. J. Tudos and R. B. M. Schasfoort, in *Chapter 1 Introduction to Surface Plasmon Resonance*, The Royal Society of Chemistry, 2008, pp. 1–14.
9 A. J. Zemann, E. Schnell, D. Volgger and G. K. Bonn, *Anal. Chem.*, 1998, **70**, 563–567.
10 J. G. A. Brito-Neto, J. A. Fracassi da Silva, L. Blanes and C. L. do Lago, *Electroanalysis*, 2005, **17**, 1198–1206.
11 J. Liu, J. Wang, Z. Chen, Y. Yu, X. Yang, X. Zhang, Z. Xu and C. Liu, *Lab Chip*, 2011, **11**, 969–973.
12 J. Gamby, J.-P. Abid and H. H. Girault, *J. Am. Chem. Soc.*, 2005, **127**, 13300–13304.
13 J. Gamby, J. P. Abid, M. Abid, J. P. Ansermet and H. H. Girault, *Anal. Chem.*, 2006, **78**, 5289–5295.
14 G. Schaumburg, *Dielectrics Newsletter, Scientific Newsletter for Dielectric Spectroscopy*, 1997, vol. 08, pp. 5–10.
15 M. Faure, M. Kechadi, B. Sotta, J. Gamby and B. Tribollet, *Electroanalysis*, 2013, **25**, 1151–1158.
16 J. S. Rossier and H. H. Girault, *Lab Chip*, 2001, **1**, 153–157.
17 Z. Wu, H. Jensen, J. Gamby, X. Bai and H. H. Girault, *Lab Chip*, 2004, **4**, 512–515.
18 M. Kechadi, J. Gamby, L. Chaal, H. Girault, B. Saidani and B. Tribollet, *Electrochim. Acta*, 2013, **105**, 7–14.
19 M. Kechadi, J. Gamby, L. Chaal, B. Saidani and B. Tribollet, *J. Flow Chem.*, 2013, **3**, 81–86.
20 M. Kechadi, L. Chaal, B. Tribollet and J. Gamby, *Analyst*, 2014, **139**, 1492–1497.
21 E. G. G. Spada and P. Giunchedi, *Proc. World Acad. Sci. Eng. Tech.*, 2011, **52**, 245–249.
22 V. Ferraro, R. F. Jorge, I. B. Cruz, P. M. L. Castro and M. E. Pintado, *J. Chem. Technol. Biotechnol.*, 2014, **89**, 671–681.
23 I. Langmuir, *J. Am. Chem. Soc.*, 1918, **40**, 1361–1403.
24 E. A. James and D. D. Do, *J.Chromatogr. A*, 1991, **542**, 19–28.
25 G. P. Jeppu and T. P. Clement, *J. Contam. Hydrol.*, 2012, **129–130**, 46–53.
26 A. Kausaite, M. van Dijk, J. Castrop, A. Ramanaviciene, J. P. Baltrus, J. Acaite and A. Ramanavicius, *Biochem. Mol. Biol. Educ.*, 2007, **35**, 57–63.